Single cell transcriptional changes across the blood stages of artemisinin resistant K13^{C580Y} mutant *Plasmodium falciparum* upon dihydroartemisinin exposure

Cliff I. Oduor[1], Clark Cunningham[2], Nazrin Rustamzade[1], Jenna Zuromski[1], Deborah M. Chin[1], Christian P. Nixon[1], Jonathan D. Kurtis[1], Jonathan J. Juliano[2,3,4+], Jeffrey A Bailey[1+*]

1. Department of Pathology and Laboratory Medicine, Brown University, Providence, RI

2. Division of Infectious Diseases, Department of Medicine, University of North Carolina, Chapel Hill, NC

3: Curriculum in Genetics and Molecular Biology, School of Medicine, University of North Carolina, Chapel Hill, NC

4: Department of Epidemiology, Gillings School of Global Public Health, University of North Carolina, Chapel Hill, NC

+: Co-senior authors

***Corresponding author:**
Jonathan J. Juliano, MD
2340 MBRB
CB#7036
111 Mason Farm Rd.
University of North Carolina
Chapel Hill, NC 27599
Tel: 919-843-5065
Email: jjuliano@med.unc.edu

ABSTRACT (200 words)

Artemisinins have been a cornerstone of malaria control, but resistance in *Plasmodium falciparum*, due to mutations in the *Kelch 13* gene, threaten these advances. Artemisinin exposure results in a dynamic transcriptional response across multiple pathways, but most work has focused on ring stages and *ex vivo* transcriptional analysis, limiting evaluation of all life cycle stages. We applied single cell RNAseq to two unsynchronized isogenic parasite lines ($K13^{C580}$ and $K13^{580Y}$) over 6 hrs after a pulse exposure to dihydroartemisinin (DHA). Transcription was altered across all stages, with the greatest occurring at the early trophozoite and mid ring stage in both lines. This response involved the arrest of metabolic processes and the enhancement of protein trafficking and the unfolded protein response. While similar, the response was enhanced in the $K13^{580Y}$ mutant, which may lead to the dormancy phenomenon upon treatment. Increased surface protein expression was seen in mutant parasites at baseline and upon drug exposure, highlighted by the increased expression of *PfEMP1* and *GARP,* a potential therapeutic target. Antibody targeting GARP maintained anti-parasitic efficacy in mutant parasites. This work provides single cell insight of gene transcription across all life cycle stages revealing transcriptional changes that could initiate dormancy state and mediate survival.

Keywords: *Plasmodium falciparum*, drug resistance, artemisinin, dihydroartemisinin, Kelch13, Single-cell, RNA-seq, Transcriptome.

INTRODUCTION

Malaria remains one of the most common infectious diseases in the world and one of the greatest global health concerns, with an estimated 247 million reported malaria cases and 619,000 malaria-related deaths in 2022 of which 76% were in children under five years[1]. *Plasmodium falciparum* (*Pf*) accounts for 99.7% of estimated malaria cases and virtually all the deaths in Africa[1]. The World Health Organization recommends artemisinin-based combination therapies (ACTs) for the treatment of uncomplicated falciparum malaria. These combinations rely on the fast-acting properties of the artemisinin derivative to rapidly clear parasites with the longer-acting partner drugs clearing residual parasites, reducing the frequent observation of recrudescent infections when artemisinin drugs are used alone[2]. Effective treatment and management of *P. falciparum* is now endangered by emerging partial resistance to artemisinin with multiple validated mutations in Africa (Rwanda, Uganda, Ethiopia, and Tanzania)[3–9], the basis of the most commonly used antimalarial therapies today, which jeopardizes the considerable gains made against malaria over the past decade. Given the vast majority of disease burden is in Africa, a public health disaster could arise if artemisinin partial resistance spreads across the continent[10,11].

Resistance to artemisinin derivatives first emerged in western Cambodia. Clinical resistance is partial to artemisinin and is expressed as a reduced rate of parasite clearance (>5 hr parasite half life), low level residual parasitemia 3 days after treatment, or increase rate or recrudescence. This resistance biologically manifests as a decreased susceptibility of ring-stage parasites and is highly attributed to nonsynonymous mutations in the ß-propeller domain of the Kelch13 (K13) protein[7,12,13]. The identification of K13 mutations as a marker of resistance has provided the impetus for a comprehensive series of studies that track and analyze the distribution of K13 mutations in malaria-endemic regions[7,14]. Over 100 different K13 mutations have been identified[15], of these, the frequently occurring mutations include C580Y, R539T, I543T, and Y493H, with the C580Y mutation being the most dominant in the Southeast Asia region[16–18]. In Eastern Africa, the mutations K13 561H, 675V, 469Y, and 622I have emerged and are now found in multiple countries. The role of K13 mutations in conferring artemisinin partial resistance has been genetically validated by reversion of mutations in clinical isolates from Cambodia and the introduction of mutations into well characterized laboratory strains *in vitro*, by selection and gene editing[13,19]. While the degree of resistance is modulated by the genetic background, K13 mutants exhibit about tenfold higher residual viability than their genetically matched wild-type parasites when exposed to dihydroartemisinin (DHA) at the early ring stage. This work has sparked intense interest in the function of K13 and its role in underpinning resistance.

K13 protein function remains to be fully understood. It consists of 726 amino acids and exhibits sequence similarity to a class of Kelch/BTB/POZ ubiquitination adaptors[12,20]. K13 protein functions within the endocytosis pathway required for hemoglobin uptake from the host cell[19], which is critical for parasite survival and ART resistance. Resistant K13 mutations in the propeller are thought to partially reduce normal function, which in turn is thought to diminish hemoglobin endocytosis. Reduced hemoglobin uptake limits the availability of hemoglobin-derived Fe2+-heme necessary for drug activation to kill the rings via alkylation of proximal proteins[20,21]. These K13 mutations mediate delayed parasite clearance following ART exposure having a reduced but still significant level of killing in resistance lines, thus skewing the focus on constitutive differences between the K13 mutant and wildtype parasites without drug exposure.

In this study, we explored the single cell transcriptomic profile of K13 580Y mutant (CamWT_C580Y, MRA-1251) and K13 C580 wildtype (CamWT, MRA-1250) *P. falciparum* isogenic lines following ART exposure for 6 hour and monitored gene expression changes every 2hrs in exposed and unexposed parasites. We observed parasite stage specific gene expression profiles and also potential vulnerabilities of the parasite's response to DHA treatment, such as elevated GARP surface protein expression, that can be a logical therapeutic target for effective combination therapies in the face of artemisinin partial resistance.

RESULTS

P. falciparum parasite stage specific transcriptional profiling and stage specific annotation

To study the transcriptomic profiles of *P. falciparum* cells in response to DHA exposure, we isolated isogenic non-synchronized wildtype ($K13^{C580}$) and mutant ($K13^{580Y}$) parasites after 48hrs in culture, and profiled the transcriptome at the single cell level at different timepoints of treatment with DHA (Figure 1). This approach allowed us to compare and contrast the transcriptional profiles of all the erythrocytic life cycle stages (merozoite, intraerythrocytic and gametocytes) in order to understand the transcriptional activity upon exposure to DHA. The top principal components (PCs) were dimensionally reduced via uniform manifold approximation (UMAP) and unsupervised clustering was performed at several resolutions to cluster *Pf* parasite cells with similar gene expression signatures (Figure 2A and Supplementary Figure S1A). To systematically identify parasite stage specific marker genes, we performed differential expression (DE) analysis by comparing the expression level in cells of one cluster to the levels in the rest of cells (Figure 2A, Table S2A). Based on the top 20 DE genes and known canonical stage specific marker genes (Figure S3A), we were able to annotate the integrated single cell clusters generated in our dataset (Figure 2A and 2B). With this single cell

dataset we were also able to identify more intraerythrocytic parasite stage-specific gene expression profiles and provide insight on gene usage at different stages of the parasite's intra-erythrocyte life cycle (Supplementary Figure S1B). As previously reported these findings suggest that the mutant parasites exhibit a longer ring phase with delayed ring to trophozoite transition (Figure 2C) compared to the wild-type. The expression profile of the mutant parasite displayed a continuous transition from one parasite stage to another compared to the wildtype strain that had more distinct gene expression patterns captured under similar conditions. This temporal data also suggest a decelerated rate of progression of the mutant parasite compared to the wildtype, as observed by the large population of trophozoites transitioning to schizonts didn't abate compared to the WT on both strains of *P. falciparum* 3D7. UMAP clustering of the wildtype and mutant separately shows the wildtype having distinctly separated clusters of the parasite stages, while the mutant showed a more continuous transition from one stage to another (Supplemental Figure S2). Overall, all parasite stages were present in both mutant and wildtype parasites.

Differential expression between untreated K13^{C580Y} mutant and K13 wild type parasite strains.

The transcriptional differences between the mutant and the wildtype strains were determined in the absence of the drug by comparing the gene expression profile of the mutant untreated control to wildtype untreated control (Figure 3). The genetic difference between mutant and wildtype parasite strains we used was verified using Molecular inversion probes targeting multiple drug resistant markers. The parasite's identity was consistent with previous genotyping and the only difference was in K13 (Figure 2C). PF3D7_1343700 (*K13*) gene expression was observed to be highly expressed in the ring stages of both the wildtype and mutant parasites compared to all the other stages (Figure 3). Despite the fact that the K13^{580Y} mutation is not known to affect transcription efficiency of the gene, gene expression comparison between the parasite strains showed *K13* transcripts to be significantly lower (log2FC=-0.92, *p*-value=2.13e-38) in the mutant compared to wildtype (Figure 3, Supplemental Table S4). This low *K13* expression was observed in the rings, and merozoite stages of the mutant (Figure 3). Since the mutant parasite is thought to be deprived of amino acids generated from hemoglobin uptake, the parasite is thought to initiate compensatory mechanisms to minimize the fitness cost associated with the partial loss of function[22]. PF3D7_1121600 (*EXP1*) has been linked to the initiation of this compensatory process[22], shows elevated expression (log2FC=1.25, p-value=6.5E-136) in the mutant relative to wildtype rings.

Impact of DHA exposure on wildtype *P. falciparum* line.

In wildtype parasites, the transcriptional response to DHA dramatically differed based on parasite stages as was determined by comparing the single cell gene expression profile of the drug treated parasites, with matched DMSO (drug vehicle) treated controls. While we observed gene expression changes across all the erythrocytic stages of development (Supplementary Table S2) for the wildtype line, the ring stage had the greatest gene expression changes with, 188, 270, and 353 genes identified as differentially expressed (DE) (p-value<0.05 and log2FC>0.4) at 2hrs, 4hrs and 6hrs after pulsed DHA exposure respectively. The genes DE and downregulated across all the treatment timepoints in the rings, were categorically associated with metabolic processes such as glycolysis (*GAPDH*), and ATP generation (Supplemental Table S2), consistent with an arrest of parasite development, as previously reported to be the effect of DHA exposure within 18h of drug exposure[23]. We observed the upregulation of genes such as *HSP70, HSP90, HSP101*, and NOT4 across all the treatment timepoints (Figure 4). We also observed the elevated expression of genes such as *PTP3, PTP4, REX1,* and *MAHRP1* which are involved in protein trafficking and export within the parasite (Figure 4, Supplemental Table S2). *K13* gene and *Kelch13* interaction candidate (KIC) genes (such as *KIC1* and *KIC5*), known to code for proteins that associate with K13, were observed to be upregulated upon DHA treatment. The elevated expression of *K13*, and some candidate interacting genes, implies that hemoglobin endocytosis is probably enhanced as a stress response and as a result enhancing drug potency within the parasite. Since DHA is mainly known to impact phenotypic changes and parasite survival mainly in the ring and trophozoite stages, we also explored gene expression changes in the trophozoite stages of the wildtype parasite at all timepoints, but we observed very few genes DE. Given this is the wild type, which is highly susceptible to 700nM of the drug, this minimal expression change may be as a result of very few trophozoite stage wildtype parasites, which may have been eliminated by the drug quickly or have rapidly transitioned through the trophozoite stage without replacement. Despite the idea that DHA action is mainly thought to act on the rings and late trophozoites, we did observe some expression changes in the merozoites, schizonts and gametocyte stages of the wildtype parasite upon drug exposure (Supplemental Table S2 and supplemental Figure S2).

Impact of DHA exposure on *P. falciparum* mutant line.

Examining the mutant line, we observed greater gene expression changes, as a result of DHA treatment, in the trophozoite and ring stages compared to all the other erythrocytic stages of development. We identified 99, 203, and 211 genes to be DE in the ring stage of the mutant strain in response to 2hrs, 4hrs and 6hrs DHA exposure respectively. Among the genes identified to be downregulated in the ring stage of the mutant were genes associated with metabolic processes such as glycolysis (GAPDH), and ATP generation, which would imply an arrest of parasite development as observed

in the wildtype line. We also observed the downregulation of GARP gene in the ring stage of the mutant strain across all timepoints of drug exposure (Supplemental Table S3 and Figure 5), but an upregulation of this gene in the trophozoite stage across all timepoints of drug exposure. We also observed elevated expression of heat shock proteins (*HSP70*, *HSP90* and *HSP101*), upregulation of genes associated with protein trafficking (*PTP3*, *PTP4*, *REX1*, and *MAHRP1*) and also upregulation of *K13* and KIC genes (such as *KIC1*, *KIC5*) (Figure 5 and Supplemental Table S3). These finding implies that the gene expression response initiated by DHA on the mutant parasite, involved the downregulation of metabolic process, upregulation of the unfolded protein response, elevated hemoglobin uptake and increased protein trafficking, which is a similar response initiated by the ring stage of the wildtype parasite strain, but a more enhanced cytoprotective response. The trophozoite stage of the mutant strain showed many gene expression changes upon drug exposure compared to the wildtype parasite. We observed 140, 93, and 222 genes to be DE in the trophozoite stage of the $K13^{580Y}$ mutant strain in response to 2hrs, 4hrs and 6hrs DHA exposure respectively. Within the trophozoite stage we also observed the upregulation of *PTP3*, *PTP4*, *EXP1* (protein trafficking), *HSP70, HSP90, HSP101* (unfolded protein response), *ApiAP2* and contrary to the rings stage observed the upregulation of GARP across all timepoints of DHA exposure. The gene expression changes in the trophozoite also appear to be associated with the restriction of metabolic process, initiation of the unfolded protein response, and elevated protein trafficking upon exposure to a lethal dose of DHA over a 6hr period.

Mutant and wildtype strain gene expression differences after treatment.

Upon DHA treatment the transcriptional response appeared to be similar for both the mutant and wildtype parasite lines. The ring stages for both mutant and wildtype lines upregulated genes associated with processes such as, unfolded protein response, and protein trafficking upon drug exposure, while genes associated with metabolic processes such as glycolysis and ATP synthesis were downregulated (Supplemental Table S4). However, there were are some differences observed between the lines upon DHA exposure, genes within the SERA gene family (PF3D7_0207600 (SERA5), PF3D7_0207500 (SERA6)) were decreased significantly (log2FC=-1.9,s, adj-*p*-value = 4.54E-06) in mutant trophozoites compared to the wildtype trophozoites (Figure 6 and Supplementary Table S4). Given SERA family genes are thought to be important in maintaining the erythrocytic cycle growth[24–26], downregulation of these genes in the mutant strains compared wildtype strains to the DHA treated wildtype, could contribute to the initiation of parasite dormancy since this could suppress parasite development. (Supplemental Table S3).

Elevated *PfGARP* expression in the mutant parasite.

GARP has recently been identified as a promising therapeutic target based on the impact of anti-GARP antibodies shown to have on the survival of the parasite[27]. The exact role and function of GARP still remains to be elucidated, however it has been reported to be restrictively expressed in the early trophozoite stage[28]. In this study we show that the PfGARP gene is expressed in more stages of the parasite's life cycle, unlike previously reported (Figure 6). However, the expression level of this gene is variable across the stages, with higher expression between the late ring to the mid. trophozoite stages (Figure 6A). We also observed variable *GARP* expression between the isogenic lines used in the study. The mutant parasite exhibited significantly higher *GARP* gene expression compared to its wildtype strain (log2FC=3.49, adj-*p*-value<0.00001) (Figure 6A and 6B). Upon treatment of both the wildtype and mutant with 700nM DHA, we observed that *GARP* expression was significantly increased in the trophozoite stage (Figure 6B). These findings and observations would imply that GARP is involved in the parasite's response to stress/drug exposure, and in this case the response seems to be more pronounced in the mutant parasite.

Anti-GARP kills K13^{580Y} mutant *in vitro*.

Since we observed *GARP* to be elevated upon DHA treatment of the K13 mutant, we hypothesized the mutant clone should still be susceptible to anti-GARP treatment as previously performed by Raj et al. 2020[27], but wanted to ensure that there was no dysfunction of membrane proteins given their general increased expression. We performed growth-inhibition assays (GIAs) using anti-GARP-A antiserum that was prepared by immunizing mice with recombinant protein[27]. Anti-GARP-A-treated parasites (both K13 mutant and wildtype) displayed a dysmorphic, pyknotic appearance on Giemsa-stained blood smears, consistent with ‘crisis’ forms that have been associated with dying or dead parasites (Figure 7). Despite our gene expression profile showing elevated *GARP* gene expression in the mutant, we didn't see a statistically significant difference in the rate of killing of the mutant strain compared to the wildtype strain, when treated with anti-GARP serum (Figure 7, Supplemental Figure S3) consistent with equivalent functionality i of the pathway leading to death in mutant and wildtype parasites.

DISCUSSION

To date *Plasmodium falciparum (Pf)* gene expression changes triggered by drug treatment have focussed on data generated on synchronized parasites and data generated from low-throughput methods. The utility of scRNAseq in P. falciparum to explore gene usage in the K13 mutant upon treatment in the presence of the other stages in intra-erythrocytic development, has not been assessed and would consider

possible interactions to minimize drug sensitivity. Here we comprehensively surveyed the molecular behavior of *P. falciparum* wildtype and mutant parasites upon DHA exposure. We utilized Seq-Well scRNAseq technique to assess the transcriptional profiles of all human life cycle stages of isogenic mutant lines during the early period of treatment with an artemisinin derivative. Our finding and analysis corroborate findings from previous transcriptome studies on *P. falciparum* response to treatment and further provides new insight into gene usage in response to drug exposure in both the mutant and wildtype. Drug response in both strains of the parasite appeared similar, however the mutant mediated an enhanced ability to respond to drug induced stress compared to the wildtype. Downregulation of the *SERA5* and 6 genes in the mutant upon DHA exposure highlights some of the changes that could lead to parasite quiescence due to slowed development. Our results show that genes involved in unfolded protein response were upregulated in both the mutant and wildtype parasite. We also revealed an increased expression of transport associated genes in the mutant compared to the wildtype when exposed to DHA as well as a striking elevated expression of *GARP*, a potential *P. f*alciparum therapeutic target[27], in the trophozoite stage of the mutant parasites upon DHA exposure, making it a viable therapeutic target candidate against the emergence of DHA resistance as a result of $K13^{C580Y}$ mutation.

Our transcriptomic analysis revealed that the untreated mutant had lower *K13* gene expression compared to the untreated wildtype. K13 is thought to aid hemoglobin endocytosis into the parasite, to be broken down as a source of amino acids to facilitate the assembly of parasite proteins and support the life of the parasite. The presence of the $K13^{580Y}$ mutation is associated with a slow rate of progression of the parasite from the ring stage to trophozoites to schizont stage compared to the wildtype (Figure 2C). This deceleration in development in the blood-stage is thought to be as a result of impaired hemoglobin uptake which is necessary to synthesize parasite protein needed for growth. The K13 function of facilitating hemoglobin entry has been shown to be aided by a complex of other proteins known as the K13 compartment proteins (KICs)[19]. During a stress response, *P. falciparum* has been shown to elevate *K13* gene and protein expression to facilitate hemoglobin entry, thereby availing an amino acid source which will be used to synthesize proteins necessary to control the stress response. Parasites exposed to DHA treatment did exhibit elevated expression of *K13* and genes coding for the KIC's mainly at the ring stages of both the wildtype and the mutant. However in the mutant strain, *K13* gene expression was lower in most of the parasite stages expressing the gene compared to the wildtype (Figure 6), despite some of the KIC genes being elevated upon DHA exposure (Supplementary Table 2 and 3). This would suggest that aside from the *K13* mutation partially impairing K13 protein function, it could also be affecting expression of the gene in the early stages of the intra-erythrocytic development.

Artemisinin and its derivatives are known to exert their antimalarial activity by generating carbon-centered radicals that cause oxidative stress and subsequent protein alkylation[20,29]. Accumulation of the alkylated proteins increases proteotoxic stress within the parasites, causing a phenotype reminiscent of that induced by heat shock[30,31], hence the observed upregulation of *HSP70* and *HSP90* in both the mutant and wildtype upon DHA treatment. This together with the elevated expression of genes associated with protein synthesis (FIKK family of genes, *HSP40*) and transcriptional activation of genes (*ApiAP2*) implies the induction of the unfolded protein response (UPR) in both parasite strains upon DHA exposure. We also observed a relatively high number of genes coding for export and trafficking proteins to be upregulated in the rings and trophozoites of both mutant and wildtype strains upon DHA exposure, which could be as a result of ER stress response[32]. Our findings show that both the mutant and wildtype share a similar gene expression response to DHA exposure, however our findings show an enhanced expression of UPR associated genes in the mutant compared to the wildtype's response, increasing the capacity of the mutant strain to quickly repair or degrade proteins damaged by artemisinin. This therefore minimizes the damaging effects caused by the accumulation of DHA in the mutant parasite. This elevated UPR in the mutant parasite coupled with the mutant having lower levels of hemoglobin endocytosis, therefore decreasing free heme-mediated artemisinin activation, mediates the mutant's tolerance to the artemisinin, leading to resistance.

GARP was recently identified as a therapeutic target[27] and previous studies have shown that the expression of *GARP* is highly restricted to the early trophozoite stage of the parasite's life cycle; however, we show that the gene is also expressed in the late ring stages and other stages of trophozoite development (Figure 6). *GARP* shares no homology with proteins of known function, it contains several complex repeat regions and its function remains to be characterized. We observed elevated expression of *GARP* gene in the mutant compared to the wildtype parasite lines before treatment, which could imply it may be as a result of compensatory processes initiated by the parasite due to the K13 mutation. While not as elevated, other surface protein transcripts show upregulation suggesting a possible general effect. Given gene expression changes can correlate with function or represent dysregulation (e.g. increased turnover), we examined whether GARP still retained function as a therapeutic target finding equivalent anti-GARP antibody killing of parasites between mutant and wildtype. This suggests GARP and likely other surface proteins maintain normal function and suggests anti-GARP therapy can be a potential addition to our limited armamentarium as an effective therapy in the face of K13 artemisinin partial resistance mutations.

Conclusion: The cellular response of the mutant and wildtype parasite is similar. Both exhibit an arrest in metabolic functions which is accompanied by elevated expression of genes associated with response to unfolded proteins and protein trafficking. However, the mutant strain mediated an enhanced ability to deal with the drug induced stress response compared to the wildtype parasite. The enhanced expression of *GARP* in the mutant compared to the wildtype, may make it more susceptible to proposed anti-GARP therapy, which would reinvigorate the fight against malaria despite the emergence of artemisinin resistance. Future studies need to explore the gene expression changes in response to DHA treatment on other K13 mutant parasites coupled with protein expression data of the differentially expressed gene. This observed artemisinin response of the parasite needs to be explored in field isolates *P. falciparum* and also in *Plasmodium vivax*, which hasn't been able to be grown or studied outside the host.

METHODS

Parasites lines and culture. The strains of parasite lines used in this study were MRA-1250 CamWT, an artemisinin susceptible fast-clearing Cambodian *P. falciparum* isolate and MRA-1251 CamWT_C580Y, also a Cambodian *P. falciparm* isolate which features a single nucleotide substitution leading to a C580Y amino acid change (MR4, BEI Resources). The *P. falciparum* parasites were maintained at 3% hematocrit in human O+ RBCs and *P. falciparum* culture media comprising RPMI 1640 (Thermo Fisher Scientific) supplemented with 0.5% (w/v) Albumax II, 50 mg/L hypoxanthine, 0.225% NaHCO3, 25mM HEPES, and 10 mg/L gentamycin. Parasites were cultured at 37 °C in 5% O2, 5% CO2, and 90% N2 [33]. The parasite lines were cultured for 48hrs before we began exposing them to DHA and DMSO.

Drug susceptibility assays. Drug stocks of dihydroartemisinin (DHA) were made in dimethyl sulfoxide (DMSO) and aliquots were stored at −20 °C. All drug assays were conducted such that the final DMSO concentration was <0.5%. Each parasite line was exposed to 700 nM DHA along with vehicle-treated 0.05% DMSO controls in independent experiments for 6hrs as illustrated in Figure 1a. Samples from each treated parasite line were collected at 2hr intervals for single cell library preparation and sequencing.

Enrichment of parasite infected RBCs. To prepare the single cell RNAseq libraries, we needed to enrich the parasite infected RBC's thus increasing chances of loading and capturing mRNA transcripts from the parasites. Our unsynchronized parasite cultures were enriched using SLOPE as previously described[34,35] with some modifications. Briefly, erythrocyte density was measured using a Cellometer Auto T4 (Nexcelom Biosciences, Lawrence, MA) and cell density adjusted to $2x10^9$ erythrocytes/mL. The 22.5Units of the lytic agent streptolysin-O (SLO) per 50µl RBCs was added in a ratio of

2 parts SLO solution to 5 parts erythrocytes. Samples were mixed well by pipetting and incubated at room temperature for 6 min. 10 volumes of 1X PBS or media (RPMI 1640 HEPES) were added and cells were centrifuged at 2,500xg for 3 min. After removal of the supernatant, cells were washed twice more with 1X PBS. Following SLO lysis, cells suspended in 1X PBS were layered onto a 60% Percoll gradient (Sigma Aldrich, St Louis, MO) and centrifuged at 1,500xg for 10 min. The top layer of Percoll was discarded while the lower cell pellet, rich in infected erythrocytes, was collected and washed twice with 1xPBS and later suspended in 200µl RPMI to be loaded into the seqwell arrays.

Single-Cell library preparation and sequencing. To capture the transcriptome of *Plasmodium* single cells and generate single cell libraries, we utilized Seq-Well, a massively parallel, low-input scRNA-seq platform[36,37]. Briefly, 10-15,000 *Pf* infected RBC's from each time point and treatment condition were loaded onto a functionalized polydimethylsiloxane (PDMS) array preloaded with uniquely barcoded mRNA capture beads (Chemgenes; Macosko-2011-10(V+)). After cells had settled into wells, the arrays were then sealed with a hydroxylated polycarbonate membrane with a pore size of 10 nm, facilitating buffer exchange while confining biological molecules (such as DNA and RNA) within each well. Following membrane-sealing, subsequent buffer exchange permitted cell lysis, mRNA transcript hybridization to beads, and bead removal before proceeding with reverse transcription. The obtained bead-bound cDNA product then underwent Exonuclease I treatment to remove excess primer before proceeding with second-strand synthesis, then PCR amplification of the cDNA product. The cDNA products were purified using the SPRIselect beads (Beckman Coulter), and were run on a Fragment analyzer (Agilent Technologies) to verify the cDNA fragment sizes to be between 0.7-2kbps. The cDNA libraries were then fragmented and amplified for sequencing using the Illumina Nextera XT DNA Library Preparation kit (Illumina, FC-131-1096) using custom primers that enabled the specific amplification of only the 3' ends. The libraries were purified, quantified, and then sequenced on a NextSeq550 system using High output 75 cycle kits (Illumina) at an average of 20,000 reads per cell. Raw read data and processed UMI count matrices from *Pf* MRA1250 and MRA1251 single cell experiments have been deposited and are publicly available through the NIH Gene Expression Omnibus database (GEO, accession #).

Single-cell transcriptome analysis. Raw reads were processed using version 2.3.0 of the Drop-seq pipeline[38], and according to the 'Drop-seq Alignment Cookbook', both found at http://mccarrolllab.com/dropseq/. Demultiplexed FASTQs were aligned to the *P. falciparum* 3D7 reference genome (PlasmoDB v.51) using STAR aligner. Individual reads were tagged with a 12bp barcode and 9bp unique molecular identifier (UMI) contained in Read 1 of each sequencing fragment. Following alignment, reads were grouped by the 12bp cell barcodes and subsequently collapsed by the 9bp UMI to

generate a gene expression count matrix. Gene expression count matrices from *Pf* MRA1250 and *Pf* MRA1251 cell line single-cell experiments (n = 7 per *Pf* cell line) were analyzed and visualized in R (v.4.0.3) using the Seurat package (v.4.0.4)[39]. Cells with less than 300 or 500 genes and UMIs detected in less than ten cells were excluded from further analysis. We then proceeded to filter out 459 multigene family genes expressed such as *vars (PfEMP1)*, *rifins* and *stevors*, retaining genes present across the different experimental conditions for each parasite line. Library size for each group in the study were internally normalized to 10,000 transcripts, log transformed and regressed on the number of UMIs per cell before dimensionality reduction and clustering. We integrated the datasets by utilizing the canonical correlation analysis ('CCA') in Seurat[40] to identify anchors/shared sources of variations between each treated and untreated groups to learn the parasite stage specific responses to DHA and DMSO treatment. Next, read data were scaled and analyzed via principal component analysis (PCA). The top PCs (n = 20) were dimensionally reduced via uniform manifold approximation (UMAP)[41] and unsupervised clustering was performed at several resolutions to identify parasite development stages and analyze differential gene expression.

A *p*-value cutoff of 0.05 was used to determine significance. For differential gene expression (DGE) between the treatment groups, a Bonferroni correction was applied to generate adjusted *p*-values. DGE analysis was done using the MAST package[42].

Growth inhibition assay on wildtype and mutant cell lines

3D7, MRA-1250, and MRA-1251 cell lines were synchronized to the ring stage by treatment with 5% sorbitol for at least three successive replication cycles and cultured to the ring stage. Parasites were diluted with O+ RBCs to 0.5-0.75% parasitemia and 2% hematocrit in incomplete media (RPMI 1640 medium containing 25 mm HEPES and 50µg/mL hypoxanthine) supplemented with 10% AlbuMax II, 48mM sodium bicarbonate, and 20µg/mL gentamycin. Anti-PfGARP scFv clone 803 was adjusted to 2mg/mL in incomplete medium and serially diluted in 50µL total volume. 50µL of diluted parasites were added to each well, resulting in the following culture conditions: 0.5-0.75% parasitemia, 1% hematocrit in RPMI 1640 medium containing 25 mm HEPES, 50µg/mL hypoxanthine, 5% AlbuMax II, 24 mm sodium bicarbonate and 10 µg/mL gentamycin in 96-well round-bottom microtiter plates. After incubation for 72 hours, blood films and/or *Plasmodium* lactate dehydrogenase (pLDH) assays were performed to assess parasitemia levels. The half-maximum inhibitory concentration (IC50) for parasite growth was determined using a four parameter logistic regression model.

Author contributions

CIO, CC, JAB, and JJJ designed the research study. CIO, CC, DC, NR, and JZ conducted the experiments. CIO analyzed the data. CIO, JAB and JJJ wrote the manuscript. CIO, CC, NR, JZ, CN, JK, JAB, and JJJ reviewed and revised the manuscript.

Acknowledgments: The following reagents were obtained through BEI Resources, NIAID, NIH: *Plasmodium falciparum*, strains CamWT, MRA-1250 and CamMT, MRA-1251, contributed by David A. Fidock.

Funding: This work was funded by the National Institute for Allergy and Infectious Diseases (K24AI134990 to JJJ; R01AI121588 and R01AI156267 to JAB and JJJ). Funds were received by the Falk Medical Research Trust Transformational Award (JK).

Data availability: All sequence data has been submitted to SRA (# pending).

References

1. Programme GM. World malaria report 2022. Published December 8, 2022. Accessed November 14, 2023. https://www.who.int/publications/i/item/9789240064898

2. Teuscher F, Gatton ML, Chen N, Peters J, Kyle DE, Cheng Q. Artemisinin□induced dormancy in plasmodium falciparum: duration, recovery rates, and implications in treatment failure. *J Infect Dis*. 2010;202(9):1362-1368.

3. Rosenthal PJ. Has artemisinin resistance emerged in Africa? *Lancet Infect Dis*. 2021;21(8):1056-1057.

4. Tacoli C, Gai PP, Bayingana C, et al. Artemisinin Resistance-Associated K13 Polymorphisms of Plasmodium falciparum in Southern Rwanda, 2010-2015. *Am J Trop Med Hyg*. 2016;95(5):1090-1093.

5. Nyunt MH, Soe MT, Myint HW, et al. Clinical and molecular surveillance of artemisinin resistant falciparum malaria in Myanmar (2009-2013). *Malar J*. 2017;16(1):333.

6. Yasri S, Wiwanitkit V. Artemisinin resistance: an important emerging clinical problem in tropical medicine. *Int J Physiol Pathophysiol Pharmacol*. 2021;13(6):152-157.

7. Ashley EA, Dhorda M, Fairhurst RM, et al. Spread of artemisinin resistance in Plasmodium falciparum malaria. *N Engl J Med*. 2014;371(5):411-423.

8. Fola AA, Feleke SM, Mohammed H, et al. Plasmodium falciparum resistant to artemisinin and diagnostics have emerged in Ethiopia. *Nat Microbiol*. 2023;8(10):1911-1919.

9. Juliano JJ, Giesbrecht DJ, Simkin A, et al. Country wide surveillance reveals prevalent artemisinin partial resistance mutations with evidence for multiple origins and expansion of sulfadoxine-pyrimethamine resistance mutations in northwest Tanzania. *bioRxiv*. Published online November 8, 2023. doi:10.1101/2023.11.07.23298207

10. Checchi F, Durand R, Balkan S, et al. High Plasmodium falciparum resistance to chloroquine and sulfadoxine-pyrimethamine in Harper, Liberia: results in vivo and analysis of point mutations. *Trans R Soc Trop Med Hyg*. 2002;96(6):664-669.

11. Roux AT, Maharaj L, Oyegoke O, et al. Chloroquine and Sulfadoxine-Pyrimethamine Resistance in Sub-Saharan Africa-A Review. *Front Genet*. 2021;12:668574.

12. Ariey F, Witkowski B, Amaratunga C, et al. A molecular marker of artemisinin-resistant Plasmodium falciparum malaria. *Nature*. 2014;505(7481):50-55.

13. Straimer J, Gnädig NF, Witkowski B, et al. Drug resistance. K13-propeller mutations confer artemisinin resistance in Plasmodium falciparum clinical isolates. *Science*. 2015;347(6220):428-431.

14. Intharabut B, Kingston HW, Srinamon K, et al. Artemisinin Resistance and Stage Dependency of Parasite Clearance in Falciparum Malaria. *J Infect Dis*. 2019;219(9):1483-1489.

15. Ménard D, Khim N, Beghain J, et al. A Worldwide Map of Plasmodium falciparum K13-Propeller Polymorphisms. *N Engl J Med*. 2016;374(25):2453-2464.

16. Witkowski B, Amaratunga C, Khim N, et al. Novel phenotypic assays for the detection of artemisinin-resistant Plasmodium falciparum malaria in Cambodia: in-vitro and ex-vivo drug-response studies. *Lancet Infect Dis*. 2013;13(12):1043-1049.

17. Klonis N, Xie SC, McCaw JM, et al. Altered temporal response of malaria parasites determines differential sensitivity to artemisinin. *Proc Natl Acad Sci U S A*. 2013;110(13):5157-5162.

18. Saralamba S, Pan-Ngum W, Maude RJ, et al. Intrahost modeling of artemisinin resistance in Plasmodium falciparum. *Proc Natl Acad Sci U S A*. 2011;108(1):397-402.

19. Birnbaum J, Scharf S, Schmidt S, et al. A Kelch13-defined endocytosis pathway mediates artemisinin resistance in malaria parasites. *Science*. Published online January 3, 2020. Accessed September 1, 2021. https://science.sciencemag.org/content/367/6473/51

20. Tilley L, Straimer J, Gnädig NF, Ralph SA, Fidock DA. Artemisinin Action and Resistance in Plasmodium falciparum. *Trends Parasitol*. 2016;32(9):682-696.

21. Meshnick SR. Artemisinin: mechanisms of action, resistance and toxicity. *Int J Parasitol*. 2002;32(13):1655-1660.

22. Mesén-Ramírez P, Bergmann B, Elhabiri M, et al. The parasitophorous vacuole nutrient channel is critical for drug access in malaria parasites and modulates the artemisinin resistance fitness cost. *Cell Host Microbe*. 2021;29(12):1774-1787.e9.

23. Mok S, Stokes BH, Gnädig NF, et al. Artemisinin-resistant K13 mutations rewire Plasmodium falciparum's intra-erythrocytic metabolic program to enhance survival. *Nat Commun*. 2021;12(1):1-15.

24. Miller SK, Good RT, Drew DR, et al. A subset of Plasmodium falciparum SERA genes are expressed and appear to play an important role in the erythrocytic cycle. *J Biol Chem*. 2002;277(49):47524-47532.

25. McCoubrie JE, Miller SK, Sargeant T, et al. Evidence for a common role for the serine-type Plasmodium falciparum serine repeat antigen proteases: implications

for vaccine and drug design. *Infect Immun*. 2007;75(12):5565-5574.

26. Thomas JA, Collins CR, Das S, et al. Development and Application of a Simple Plaque Assay for the Human Malaria Parasite Plasmodium falciparum. *PLoS One*. 2016;11(6):e0157873.

27. Raj DK, Das Mohapatra A, Jnawali A, et al. Anti-PfGARP activates programmed cell death of parasites and reduces severe malaria. *Nature*. 2020;582(7810):104-108.

28. López-Barragán MJ, Lemieux J, Quiñones M, et al. Directional gene expression and antisense transcripts in sexual and asexual stages of Plasmodium falciparum. *BMC Genomics*. 2011;12:587.

29. Paloque L, Ramadani AP, Mercereau-Puijalon O, Augereau JM, Benoit-Vical F. Plasmodium falciparum: multifaceted resistance to artemisinins. *Malar J*. 2016;15:149.

30. Morano KA, Grant CM, Moye-Rowley WS. The response to heat shock and oxidative stress in Saccharomyces cerevisiae. *Genetics*. 2012;190(4):1157-1195.

31. Roti Roti JL. Cellular responses to hyperthermia (40-46 degrees C): cell killing and molecular events. *Int J Hyperthermia*. 2008;24(1):3-15.

32. Marti M, Spielmann T. Protein export in malaria parasites: many membranes to cross. *Curr Opin Microbiol*. 2013;16(4):445-451.

33. Schuster FL. Cultivation of plasmodium spp. *Clin Microbiol Rev*. 2002;15(3):355-364.

34. Brown AC, Guler JL. SLOPE: A two-part method for the enrichment of ring stage Plasmodium falciparum parasites. *bioRxiv*. Published online November 20, 2018:474338. doi:10.1101/474338

35. Brown AC, Moore CC, Guler JL. Cholesterol-dependent enrichment of understudied erythrocytic stages of human Plasmodium parasites. *Sci Rep*. 2020;10(1):1-15.

36. Gierahn TM, Wadsworth MH 2nd, Hughes TK, et al. Seq-Well: portable, low-cost RNA sequencing of single cells at high throughput. *Nat Methods*. 2017;14(4):395-398.

37. Aicher TP, Carroll S, Raddi G, et al. Seq-Well: A Sample-Efficient, Portable Picowell Platform for Massively Parallel Single-Cell RNA Sequencing. *Methods Mol Biol*. 2019;1979:111-132.

38. Macosko EZ, Basu A, Satija R, et al. Highly Parallel Genome-wide Expression Profiling of Individual Cells Using Nanoliter Droplets. *Cell*. 2015;161(5):1202-1214.

39. Butler A, Hoffman P, Smibert P, Papalexi E, Satija R. Integrating single-cell transcriptomic data across different conditions, technologies, and species. *Nat Biotechnol*. 2018;36(5):411-420.

40. Stuart T, Butler A, Hoffman P, et al. Comprehensive Integration of Single-Cell Data. *Cell*. 2019;177(7):1888-1902.e21.

41. Becht E, McInnes L, Healy J, et al. Dimensionality reduction for visualizing single-cell data using UMAP. *Nat Biotechnol*. Published online December 3, 2018. doi:10.1038/nbt.4314

42. Finak G, McDavid A, Yajima M, et al. MAST: a flexible statistical framework for assessing transcriptional changes and characterizing heterogeneity in single-cell RNA sequencing data. *Genome Biol*. 2015;16:278.

Figures

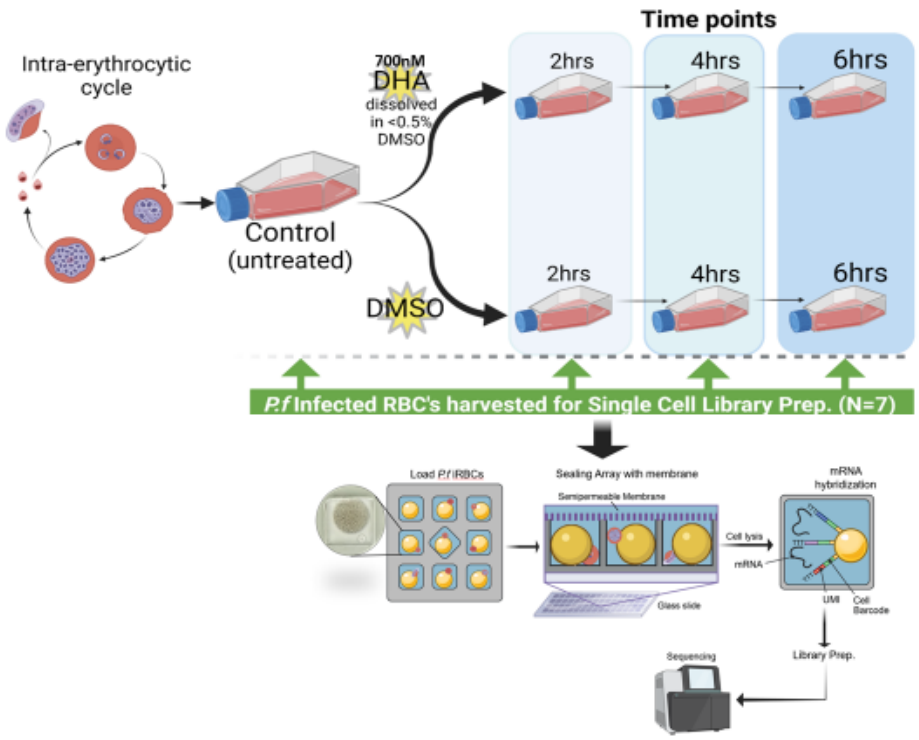

Figure 1: Schema of the experimental workflow applied in this study to explore transcriptome changes upon DHA exposure. This schematic diagram illustrates the study design, points of sample collection and treatment, sample processing and single cell library preparation using the Seq-Well platform. Both the wildtype ($K13^{C580}$ strain) and mutant ($K13^{580Y}$ mutant strain) *Pf* parasite cell lines were cultured separately for 48hrs. The control (untreated) parasite was collected for library prep. The controls for each parasite strain were then divided into two groups, some treated with 700 nM DHA (lethal dose of DHA) and DMSO. After DHA and dmso treatment or exposure, samples were collected after every 2hrs for single cell library preparation using Seq-Well

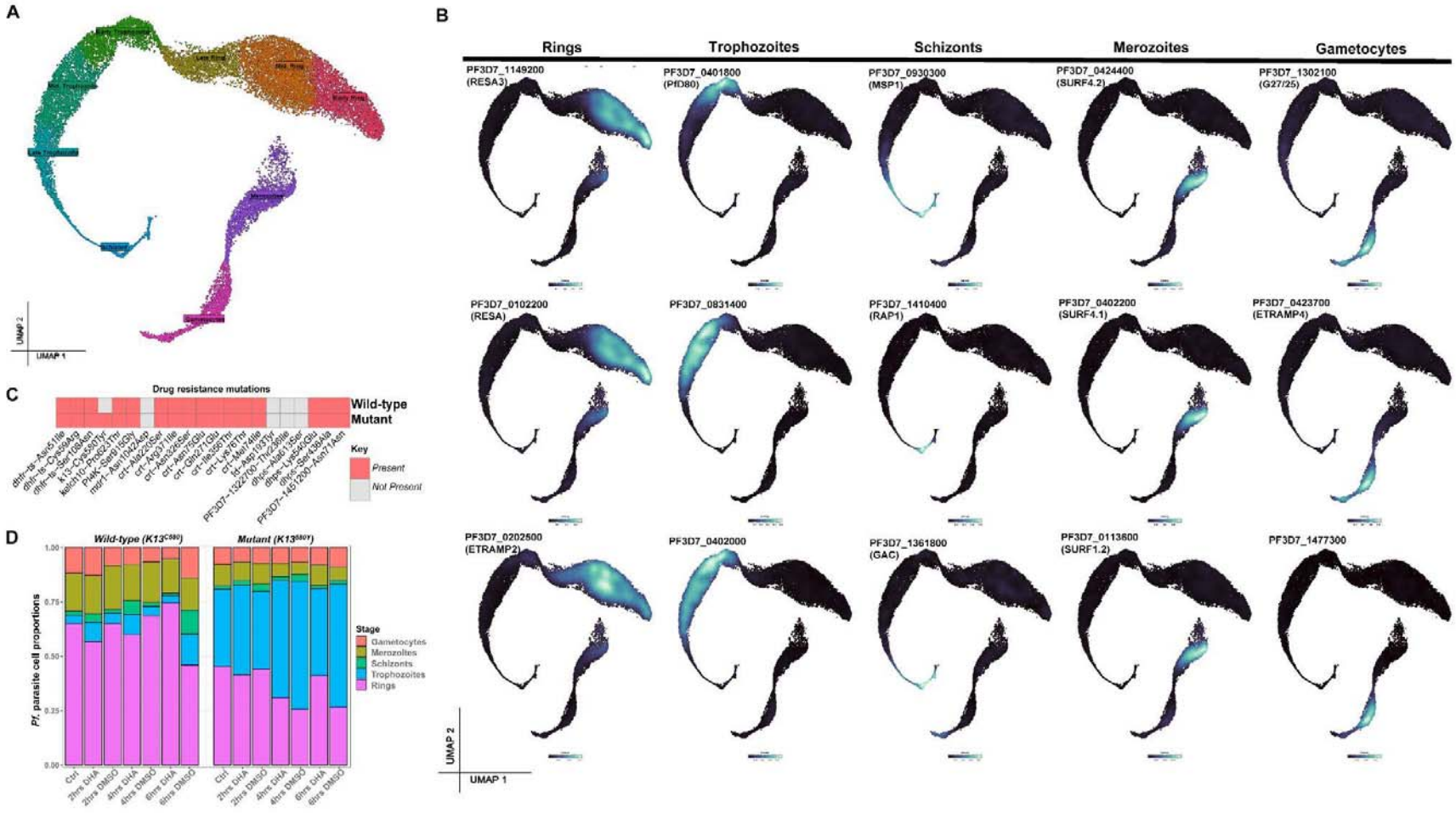

Figure 2: Single-cell gene expression identifies distinct life-cycle stages. A. UMAP of single-cell transcriptomes sampled from all stages of the life cycle, with cells colored according to their stage. **B**. UMAP representations displaying the expression of parasite stage specific gene expression markers. With this single-cell gene expression profile of the *Pf* parasite we can identify new unknown stage specific parasite marker genes. **C**. Presence and absence of known drug resistant mutations between the two PF3D7 parasite strains (mutant and wildtype). We validated that the only variant difference between the two strains used in this study was the $K13^{C580Y}$ mutation is only present in the mutant strain. **D.** Distribution of parasite developmental stages across all sample groups (Untreated controls, DHA and DMSO treated parasites).

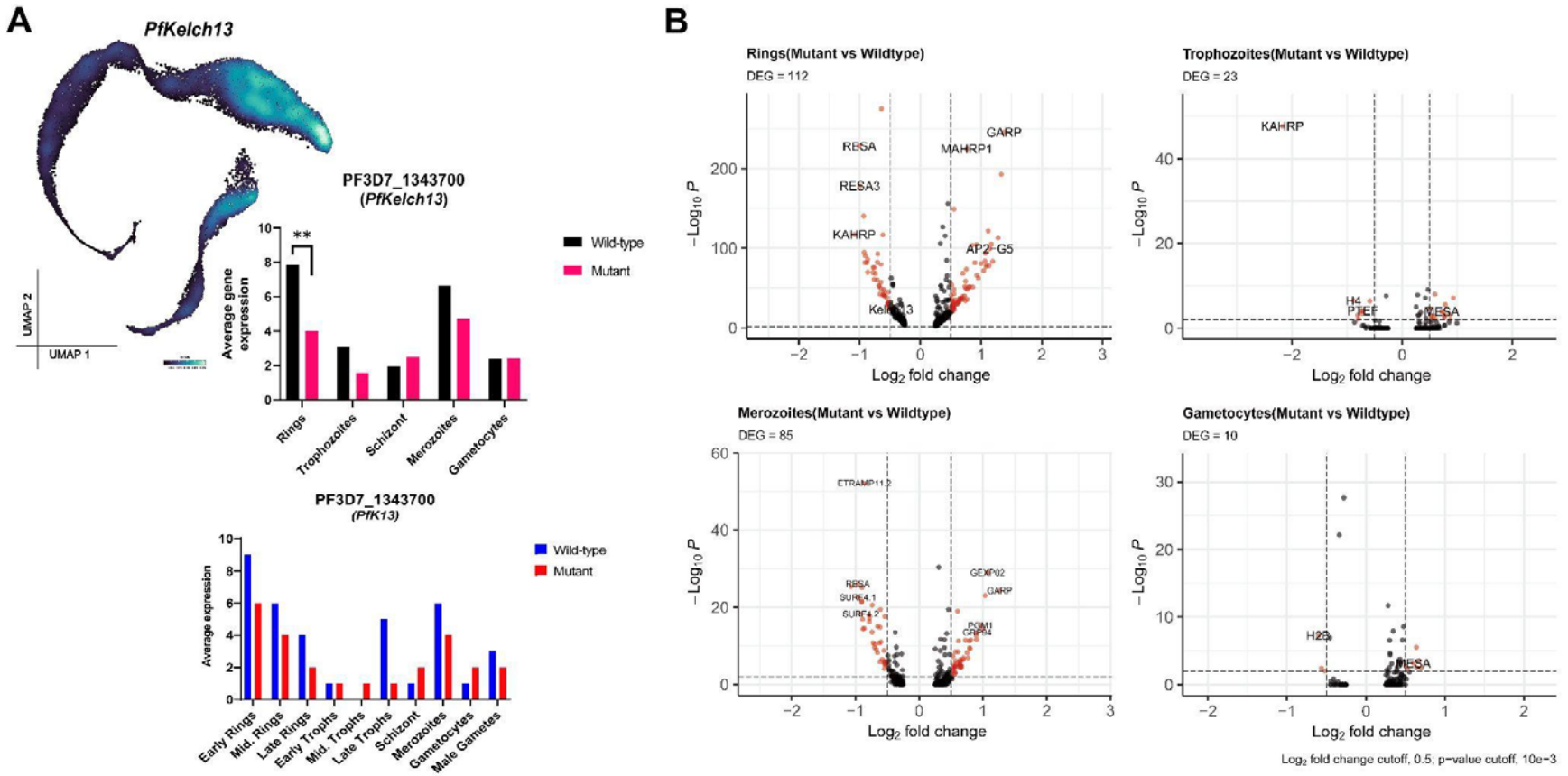

Figure 3: Gene expression differences between mutant and wildtype parasites. A. *Kelch13* gene expression was observed to be downregulated in the mutant parasite population compared to the wildtype parasite (BH-adjusted p-value<0.01 and log2FC=1.5). *PfKelch13* gene expression across the parasite stages in each strain, shows *PfKelch13* gene to be highly expressed in the wildtype across all the stages compared to the mutant parasite. **B**. Volcano plot showing DEGs in the untreated mutant compared to untreated wildtype on different parasite stages. Each red dot denotes genes differentially expressed between the wildtype and the mutant (such as *GARP* and *MAHRP1* which are upregulated in the mutant rings compared to WT rings).

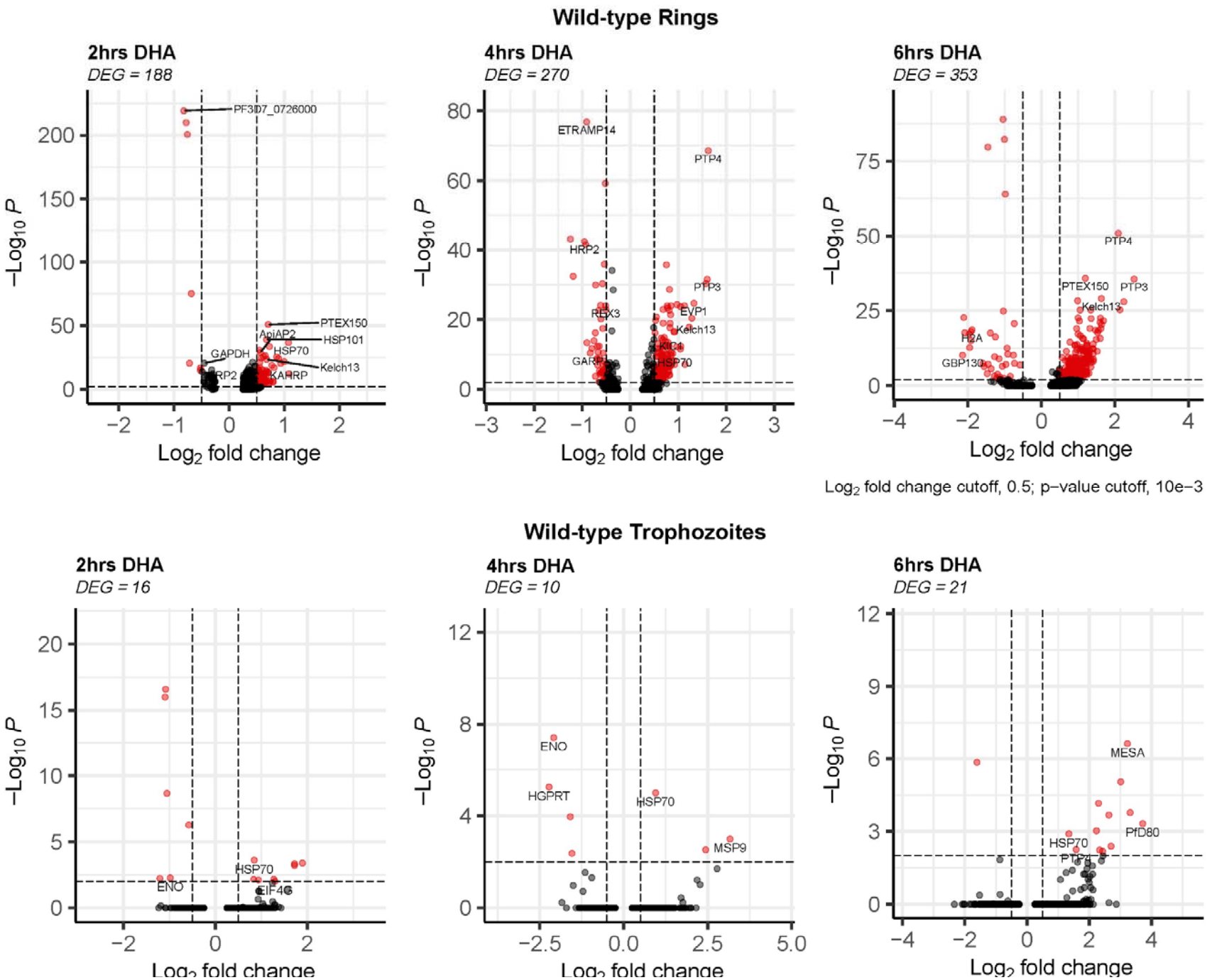
Wild-type Rings
2hrs DHA
DEG = 188
PF3D7_0726000
PTEX150
ApiAP2
HSP101
HSP70
GAPDH
Kelch13
KARRP
4hrs DHA
DEG = 270
ETRAMP14
PTP4
HRP2
PTP3
REX3
EVP1
Kelch13
HSP70
6hrs DHA
DEG = 353
PTP4
PTEX150
PTP3
Kelch13
H2A
GBP130
−Log10 P
Log2 fold change
Log2 fold change cutoff, 0.5; p−value cutoff, 10e−3
Wild-type Trophozoites
2hrs DHA
DEG = 16
HSP70
ENO
EIF4G
4hrs DHA
DEG = 10
ENO
HGPRT
HSP70
MSP9
6hrs DHA
DEG = 21
MESA
PfD80
HSP70

Figure 4: Gene expression differences associated with wildtype (Rings and Trophozoites) DHA response. Volcano plot showing DEGs in *Pf* K13wt DHA treated versus K13wt DMSO treated (control) at 3 different timepoints. Each red dot denotes genes passing P value and fold change difference (BH-adjusted p-value<0.01, average log2 fold-change >0.3) thresholds, those on the right side of the plots are the upregulated genes induced due to DHA exposure. The red dots on the left side of the plots represent the downregulated genes passing the p-value and fold change difference between the DHA treated parasite and the DMSO treated parasite control (BH-adjusted p-value<0.05, average log2 fold-change <-0.3).

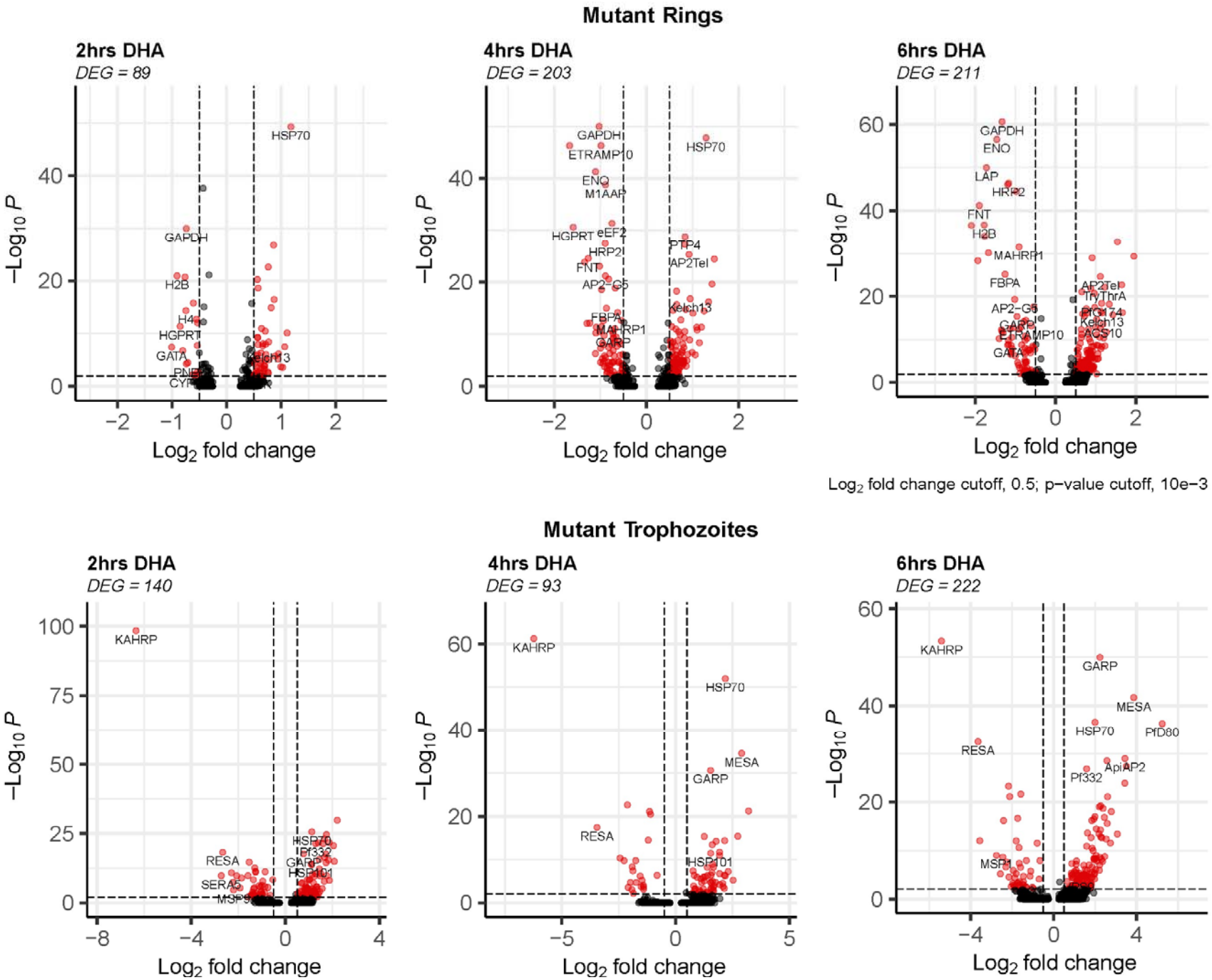
Mutant Rings
2hrs DHA
DEG = 89
HSP70
GAPDH
H2B
H4
HGPRT
GATA
Kelch13
4hrs DHA
DEG = 203
GAPDH
ETRAMP10
ENO
M1AAP
HGPRT
eEF2
HRP2
FNT
AP2-G5
FBPA
MAHRP1
GARP
HSP70
PTP4
AP2Tel
Kelch13
6hrs DHA
DEG = 211
GAPDH
ENO
LAP
HRP2
FNT
H2B
MAHRP1
FBPA
AP2-G5
GARP
ETRAMP10
GATA
AP2Tel
TryThrA
PfG174
Kelch13
ACS10
−Log10 P
Log2 fold change
Log2 fold change cutoff, 0.5; p−value cutoff, 10e−3
Mutant Trophozoites
2hrs DHA
DEG = 140
KAHRP
RESA
SERA5
MSP9
HSP70
Pf332
GARP
HSP101
4hrs DHA
DEG = 93
KAHRP
HSP70
MESA
GARP
RESA
HSP101
6hrs DHA
DEG = 222
KAHRP
GARP
MESA
HSP70
PfD80
RESA
ApiAP2
Pf332
MSP1

Figure 5: Gene expression differences associated with mutant (Rings and Trophozoites) response to DHA treatment *in vitro*. Volcano plot showing DEGs in *Pf* K13^{580Y} mutant treated with DHA versus K13^{580Y} mutant parasite treated with DMSO (control) at 3 different timepoints. Each red dot denotes genes passing P-value and fold change difference (BH-adjusted p-value<0.05, average log2 fold-change >0.3) thresholds, those on the right are the upregulated genes induced due to DHA exposure. The red dots on the left represent the downregulated genes passing the p-value and fold change difference thresholds between the DHA treated parasite and the DMSO treated parasite control (BH-adjusted p-value<0.01, average log2 fold-change <-0.3).

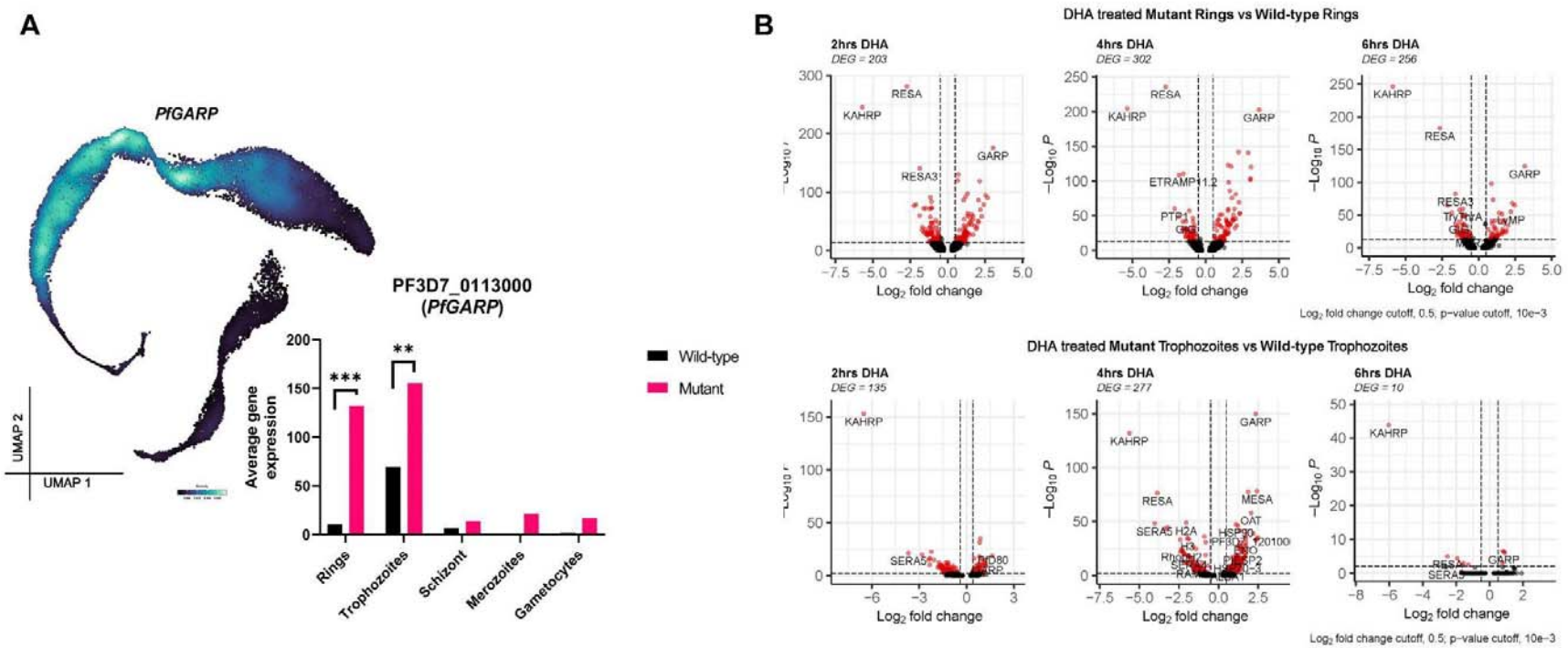

Figure 6: Gene expression differences between DHA treated mutant and wildtype parasites. A. *PfGARP* was observed to be highly expressed in the mutant parasite population compared to the wildtype parasite population (BH-adjusted p-value<0.01 and log2FC=3.8). Stratifying the *PfGARP* expression across the parasite stages in each strain, shows *PfGARP* to be highly expressed in the mutant across all the stages compared to the wildtype parasite. **B**. Volcano plot showing DEGs in the mutant treated with DHA versus wildtype parasites also treated with DHA at 3 different timepoints. Each red dot denotes genes passing P-value and fold change difference (BH-adjusted p-value<0.05, average log2 fold-change >0.3) thresholds, the dots on the right are the upregulated genes induced due to DHA exposure. The red dots on the left represent the downregulated genes passing the p-value and fold change difference thresholds between the DHA treated parasite and the DMSO treated parasite control (BH-adjusted p-value<0.01, average log2 fold-change <-0.3.

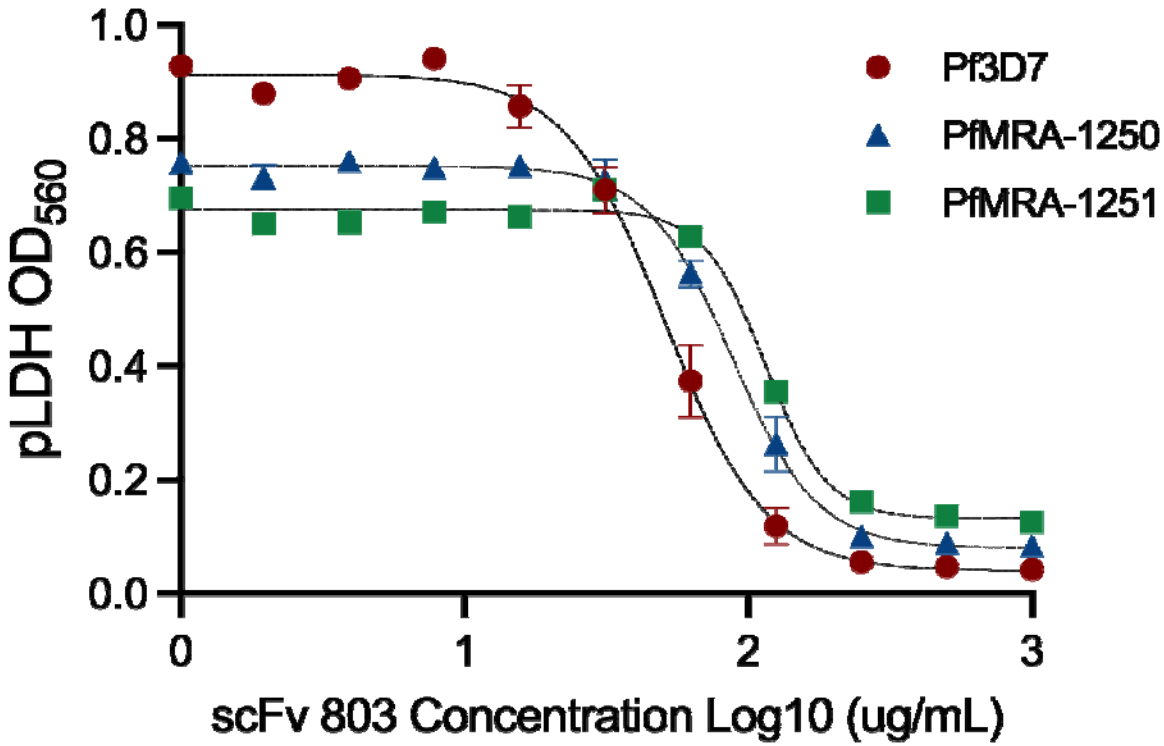

Figure 7: Anti-PfGARP mAb clone 803 kills both mutant and wildtype parasites *in vitro*. Ring-stage *P. falciparum* parasite strains Pf3D7, PfMRA-1250, and PfMRA-1251 were incubated for 72 hours with serially diluted anti-PfGARP scFv antibody clone 803 or media only. Parasitemia was evaluated by pLDH assay. Antibody treatment resulted in significant parasite growth inhibition. Data was fit to a four parameter logistic regression model to obtain the following IC50 values: Pf3D7= 50µg/mL, PfMRA-1250= 87µg/mL, and PfMRA1251= 114µg/mL. Data points represent the mean of two (PfMRA-1250) or three (Pf3D7 and PfMRA-1251) biologically independent replicates, with error bars indicating SEM.

** 2 experimental repeats have been executed with Pf3D7 and PfMRA-1250
*** 0 experimental repeats for PfMRA-1251

Supplemental Figures and Tables.

Single cell transcriptional changes across the blood stages of artemisinin resistant K13^{C580Y} mutant *Plasmodium falciparum* upon dihydroartemisinin exposure

Cliff I. Oduor[1], Clark Cunningham[2], Nazrin Rustamzade[1], Jenna Zuromski[1], Deborah M. Chin[1], Christian P. Nixon[1], Jonathan D. Kurtis[1], Jonathan J. Juliano[2,3,4+], Jeffrey A Bailey[1+*]

1. Department of Pathology and Laboratory Medicine, Brown University, Providence, RI

2. Division of Infectious Diseases, Department of Medicine, University of North Carolina, Chapel Hill, NC

3: Curriculum in Genetics and Molecular Biology, School of Medicine, University of North Carolina, Chapel Hill, NC

4: Department of Epidemiology, Gillings School of Global Public Health, University of North Carolina, Chapel Hill, NC

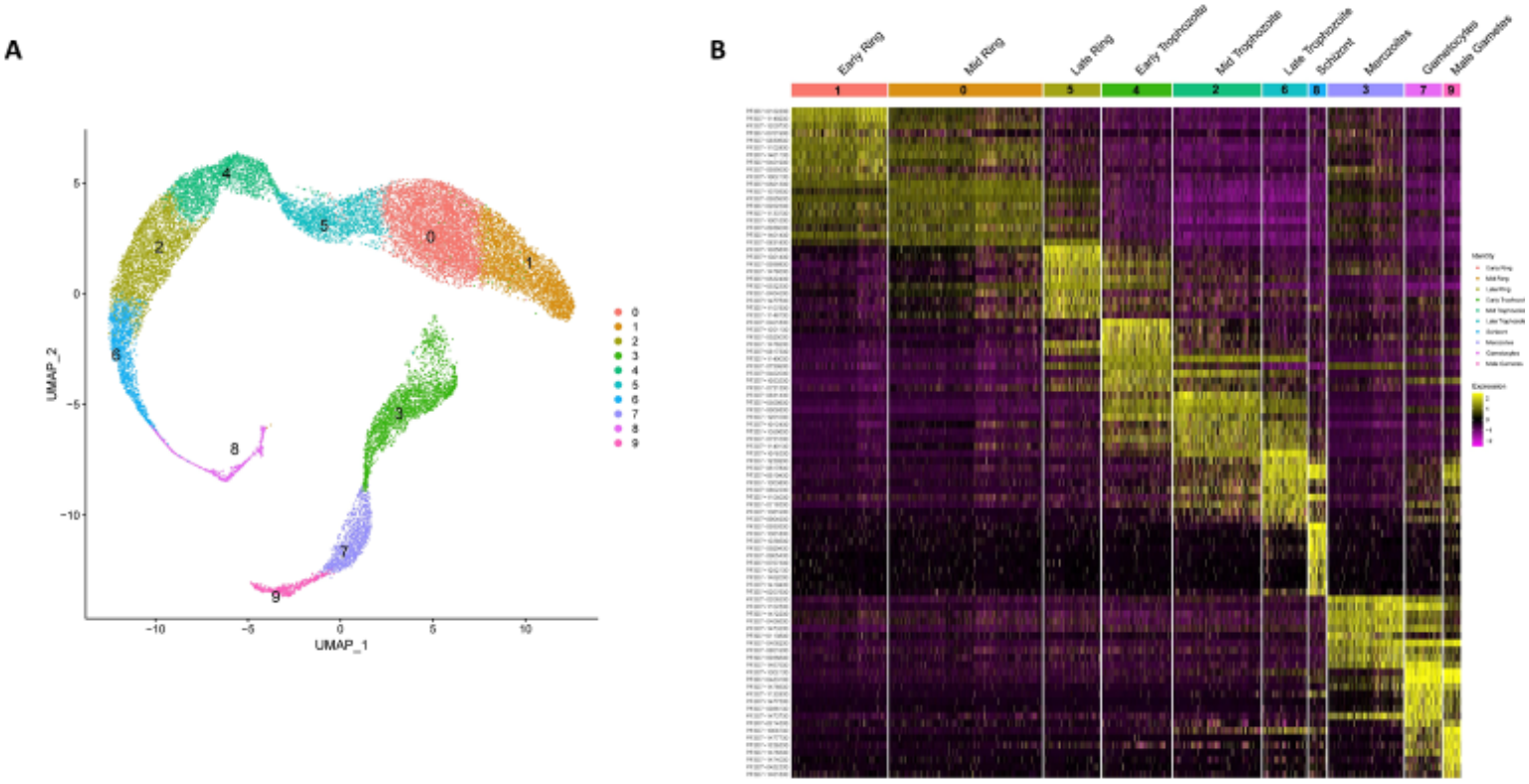

Supplementary Figure S1- A.) UMAP plot of cell clusters generated before annotating clusters. B.) Heatmap showing top 50 genes enriched in each cell cluster which identifies stage specific gene expression profile. The cells in the heatmap are ordered by their developmental progression.

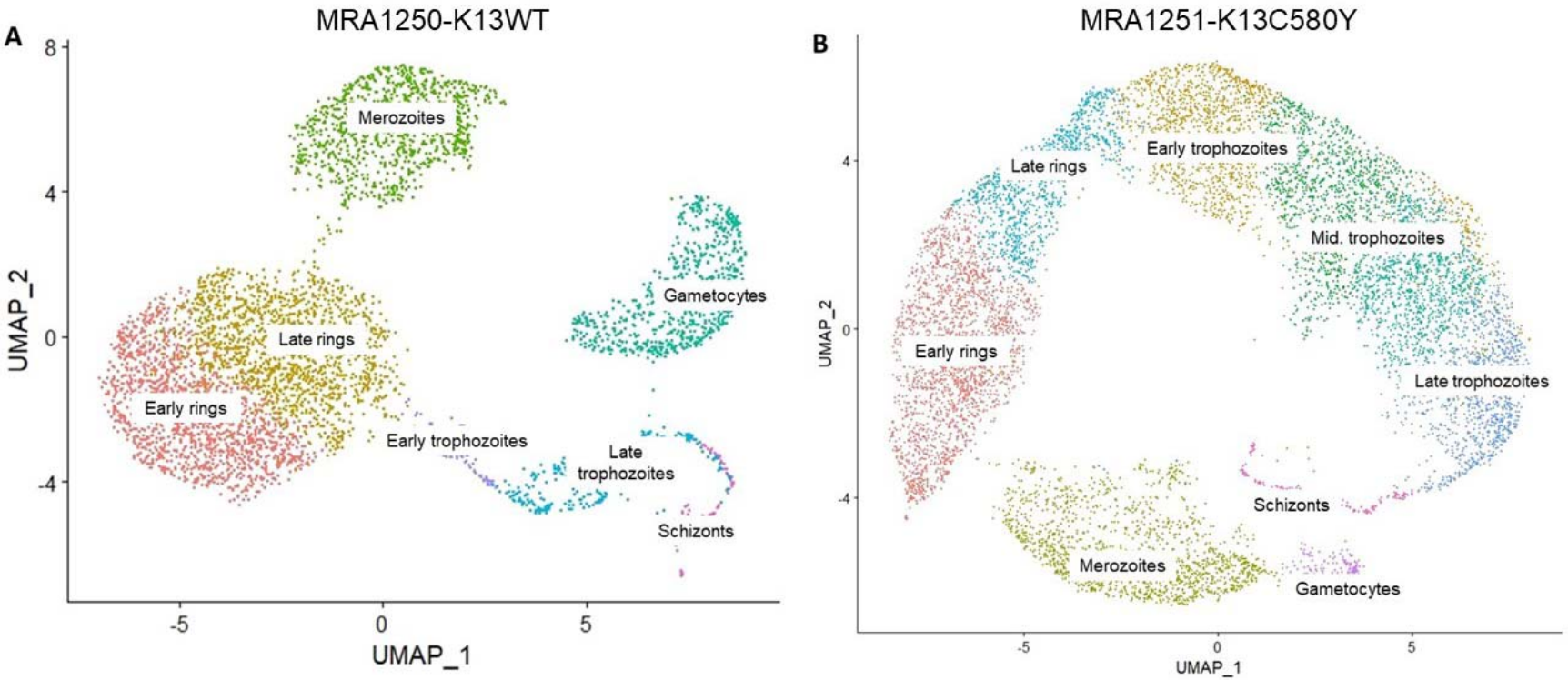

Supplementary Figure S2: UMAP projection plots of wildtype and mutant untreated *Pf* parasites.

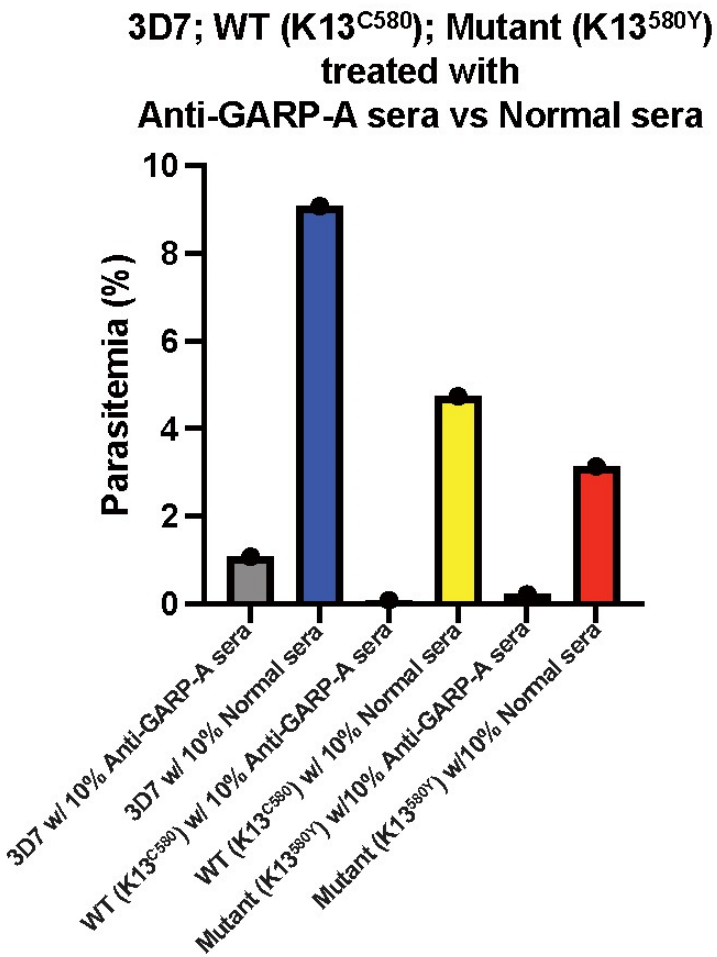

Supplementary Figure S3: Anti-PfGARP mAb kills both mutant and wildtype parasites *in vitro*.

Supplementary Table S1- Top 50 genes enriched in each *P. falciparum* single cell cluster. Gene expression profile associated with parasite stages.

Supplementary Table S2- Genes differentially expressed between the DHA treated Wildtype and the DMSO treated Wildtype parasite over the course of 6hr DHA treatment.

Supplementary Table S3- Genes differentially expressed between the DHA treated Mutant and the DMSO treated Mutant parasite over the course of 6hr DHA treatment.

Supplementary Table S4- Genes differentially expressed between the DHA treated Mutant and the DHA treated Wildtype parasite over the course of 6hr DHA treatment.